Supporting Information

CREIM: Coffee Ring Effect Imaging Model for Monitoring Protein Self-Assembly *in Situ*

Shaw et al

Materials and methods

CREIM experimental design.

Pinning of the droplet-substrate contact line combined with evaporation results in radial capillary flow in drying liquid droplets. In a suspension, this flow drives suspended particles out to the droplet edge forming a high concentration ring of particles (monomers). The velocity of this outward flow depends upon the droplet radius, R, and the droplet contact angle, θ_c (Fig 1). The mass of solute particles within the ring region, $M(R,t)$, increases exponentially according to $M(R,t) \propto t^{2/(1+\lambda)}$, where $\lambda = (\pi - 2\theta_c)/(2\pi - 2\theta_c)$, which leads to an exponential increase in concentration as a function of time. [18]

Non-hierarchical material (fluorescent microspheres): it is possible to measure the time-dependent mass of the ring of solute which forms at the edge of a drying sessile droplet by performing time-lapse imaging and counting the number of particles in the ring as a function of time.[18] The mass in the ring is expected to increase according to

$$M(R,t) \propto t^{\frac{2}{1+\lambda}}$$

where λ is dependent on the droplet contact angle according to

$$\lambda = (\pi - 2\theta_c)/(2\pi - 2\theta_c)$$

Therefore a log-log plot of ring mass (no. particles) versus time should yield a straight line with a gradient, g, of 2/(1+λ). If λ and the initial ring mass $M(R,0)$ are known, we can estimate the ring mass at a time, *t*.

$$M(R,t) = M(R,0)t^{\frac{2}{1+\lambda}}$$

If the droplet volume is maintained at the edge of the droplet then the concentration at the periphery also increases exponentially with time

$$C(R,t) = C(R,0)t^{\frac{2}{1+\lambda}}$$

To measure the exponent, crimson microspheres of 1 μm in diameter (Fluospheres, Invitrogen, stock solution diluted at 1:100) were imaged in water droplets (5 μL) added to centre of one well in an 8 well LabTek chambered cover slide (the same sample chamber was used for FiM). Following equilibration, time-lapse images were recorded in the course of drying (~ 30 mins at ~ 23°C) (Fig S2A). The accumulation of fluorescent microspheres was imaged in a plane at the droplet periphery using a 60x/1.49 objective lens with a depth of field of approximately 0.4 μm.

The number of microspheres per image was determined using ImageJ's 'Analyse Particles' function. First, the background (rolling ball radius 50 pixels) was subtracted and images binarised with auto local thresholding (Bernsen, 15 pixel radius), following by separating particles, which are touching, using watershed segmentation and counting the number of microspheres in each image frame ('Analyze Particles' function with suitable bounds for particle size and circularity). Second, the number of particles in each image frame was also counted using ImageJ's 'Find Maxima' function applied to intensity normalised, background corrected images. The measured number of particles versus time was fitted to a simple exponential function by non-linear least squares fitting in Matlab:

$$I(t) = I_0 e^{bt},$$

where $\sqrt{I}$ was used for the fitting weights (based on signal to noise ratio for a shot noise limited system). The analysis by gave b = 0.00190 with 95% confidence bounds of 0.00172 - 0.002088 and R-square of 0.96 (Fig S3).

FiM assembly by CREIM: this simplified scenario allows to estimate initial increases in monomer concentrations (n < n*) in the drying droplet (Fig 1). As filaments start forming (n* to n > n*) the flow (i) is disrupted with contributions from filament-localised Marangoni eddies[21,31] and (ii) monomers become

rapidly depleted. The amount of peptide material remains constant, but increases exponentially in the contact line, which the above model accurately describes (Fig S2). Therefore, the expression of increasing peptide concentrations is not deemed appropriate for self-assembling systems in CRE as it encompasses both monomeric (passive) and filament (active) assembly phases, which indicates that CRE converts static *in vitro* measurements into hydrodynamic measurements without affecting hierarchical transformations or introducing an environmental bias. The effect thus effectively modulates the conditions under which protein assembly is driven to completion.

For each experiment, a drop of aqueous peptide solution was deposited in the centre of one well of an eight well chambered cover slide (Lab-TEK II, Nunc). Time lapse images were acquired with a camera exposure time of 50 ms per raw image, giving a maximum possible super-resolution frame rate of 2.2 frames per second. In practice, a delay (between five seconds and one minute) was added between image acquisition time points to reduce photobleaching during extended time lapse imaging. To capture end point images, following complete drying of the droplet, additional MOPS buffer was added to rehydrate the peptide.

Imaging and image analysis: all images were captured using a custom-built structured illumination microscope developed for high speed time-lapse fluorescence imaging.[29] Sinusoidal excitation patterns were generated using a spatial light modulator (SLM) configured to display binary phase gratings. A spatially filtered image of the SLM, illuminated with collimated laser light, was projected through the rear illumination port of an inverted microscope body (IX71, Olympus) and into the focal plane of the microscope objective lens (UPLSAPO 60x/1.3, Olympus). Sample images were acquired using a scientific CMOS camera (ORCA-Flash4.0, Hamamatsu Photonics), with the global exposure period of the camera's rolling shutter synchronised to the pattern displayed on the SLM. Each super resolution image was reconstructed from a sequence of nine raw images of the sample acquired under excitation with different sinusoidal irradiance patterns: three pattern orientations each separated by 60° and three pattern phases, separated by $2\pi/3$, per orientation. Reconstructions were performed as described elsewhere,[30] with out of

focus light suppressed by multiplication of the zero and first order Fourier space passbands by Gaussian and complimentary inverted Gaussian functions.

The quantification of growth kinetics was performed as described previously.[27] Briefly, time lapse images were first spatially registered to correct lateral drifts using the ImageJ plugin StackReg. Individual filament were then segmented and tracked backwards through the image sequence using open active contours implemented in the ImageJ plugin JFilament. For clarity, a smoothing spline was fitted to the resulting fibre growth curve using the MATLAB curve fitting toolbox (MathWorks). Statistical analysis was performed in MATLAB Release 2015b (Mathworks Inc.) using a two-sided t-test with unequal variances and a two-sided Wilcoxon rank sum test for each experiment in each droplet done at least in quintuplicate.

Peptide design: FiM is a symmetrical sequence of two oppositely charged α-helical modules, each comprising two heptads (Fig S1A). The sequence folds into a coiled-coil stagger that self-propagates longitudinally with the formation of protein filaments. The design is inspired by canonical coiled-coil sequences that use a heptad repeat pattern of hydrophobic (*H*) and polar (*P*) residues, *PHPPHPP*. This pattern is normally designated *gabcdef*, where *a* and *d* form hydrophobic interfaces and *g* and *e* of successive heptads (*g-e'* pairs) arrange complementary electrostatic interactions supporting an axial stagger of individual helices (Fig S1A). The solvent exposed *b*, *c* and *f* sites are not involved in the assembly directly, but impact on the resulting fibre morphology. The hydrophobic interfaces were made leucines, which stabilise homotrimer formation, though at the expense of specificity. As a result, mixed interfacial interactions featuring also dimer formation introduce a conflict that loosens electrostatic interactions allowing *g-e*' pairs to re-engage in the assembly. Unengaged electrostatic pairs make filament surfaces highly polar disfavouring fibre thickening. Because all pair re-engagements are concomitant along the aligned sequences such changes in the electrostatic network of each filament are deemed cooperative.[27]

Peptide preparation: all the peptides were assembled on a Liberty microwave peptide synthesizer (CEM) using standard Fmoc/tBu solid-phase protocols with HBTU/DIPEA as coupling reagents on a Fmoc-Glu(OtBu)-Wang resin for FiM and FiM Alexa Fluor 488 and an MBHA Rink amide resin for FiMs .

Fmoc-Lys(Alloc)-OH was used for the orthogonal coupling of Alexa Fluor 488 to the peptide. FiMs has two identical subunits that were assembled simultaneously via two tri-β-alanyl linkers attached to α-amino and ε-amino groups of a lysine on the resin. After cleavage and deprotection (95% TFA, 2.5% TIS, 2.5% water) peptides were purified using RP-HPLC and their purities were confirmed by analytical RP-HPLC. Analytical and semi-preparative gradient RP-HPLC were performed on a JASCO HPLC system using Vydac C_{18} analytical and semi-preparative (5 μm) columns. All runs used a 10−70% B gradient over 40 min at 1 mL/min (analytical) and 4.7 mL/min (semi-preparative) with detection at 230 and 220 nm (buffers A and B are 5% and 95% aqueous CH_3CN containing 0.1% TFA, respectively). Peptide identities were confirmed by analytical RP-HPLC and MALDI-ToF. Table S1.

Assembly conditions: peptide solutions (200 μL, 300 μM total peptide) were prepared in filtered (0.22 μm) 10 mM aq. MOPS (or phosphate buffer), pH 7.4, at the molar ratios stated: FiM with FiM-Alexa Fluor 488 ($1:10^{-3}$), FiM:FiM-Alexa Fluor 488 ($1:10^{-3}$) with FiMs at 1:0.5; FiM:FiM-Alexa Fluor 488 ($1:10^{-3}$) with FiMs at $1:10^{3}$. Enhanced GFP (1 mg/mL in phosphate buffer, MBL International) used as a non-assembling control was reconstituted to 10 μg/mL in filtered (0.22 μm) 10 mM phosphate buffer (5μL).

Table and Figures

Table S1. Peptides used in the study

Name	Amino-acid sequence	MS $[M+H]^+$, m/z	
		calc.	found
FiM	KLAALKQKLAALKKELAALEQELAALEQ	3033.6	3036.5
FiM-Alexa Fluor 488*	KLAALKQKLAALK**K**ELAALEQELAALEQ	3555.6	3557.1
FiMs	$(KLAALKQKLAALKQ\beta A\beta A\beta A)_2$K-am	3583.5	3587.8

*attachment site for Alexa Fluor 488 is shown in bold

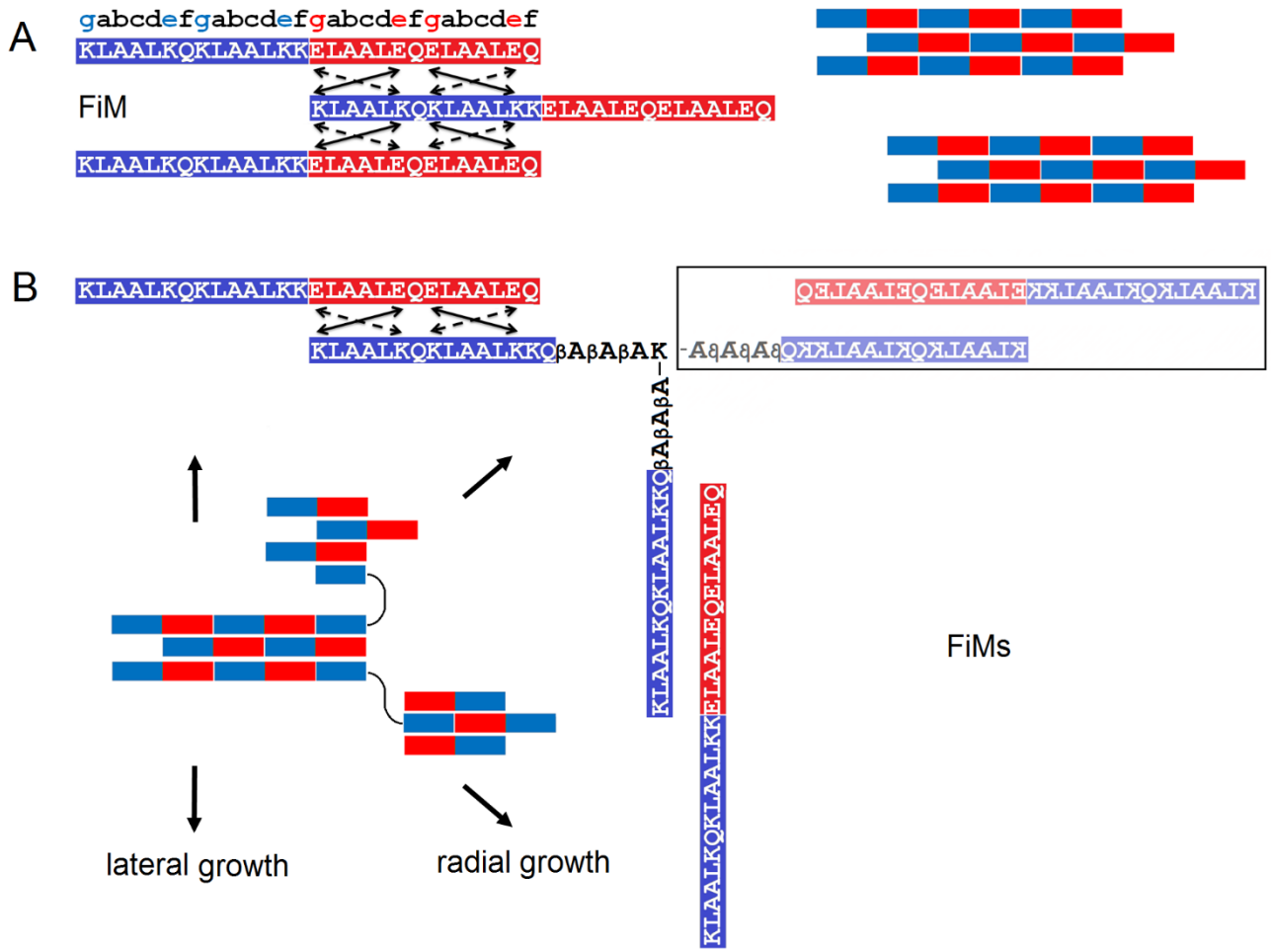

Figure S1. **Filamentous α-helical assembly model**. (A) The standard FiM assembl. Key: cationic (blue) modules and complementary to anionic (red) modules with corresponding amino-acid sequences are shown as N- and C-terminal domains, respectively; arrows indicate electrostatic interactions between Lys and Glu residues. The oppositely charged domains of different monomers co-fold into α-helical coiled coils that propagate longitudinally. For simplicity, only two growing filaments are schematically shown (right). (B) A complementary star-like (FiMs) assembly mode. Due to the flexible linker two N-terminal domains can bind at an angle, including a straight version (dimmed in square).

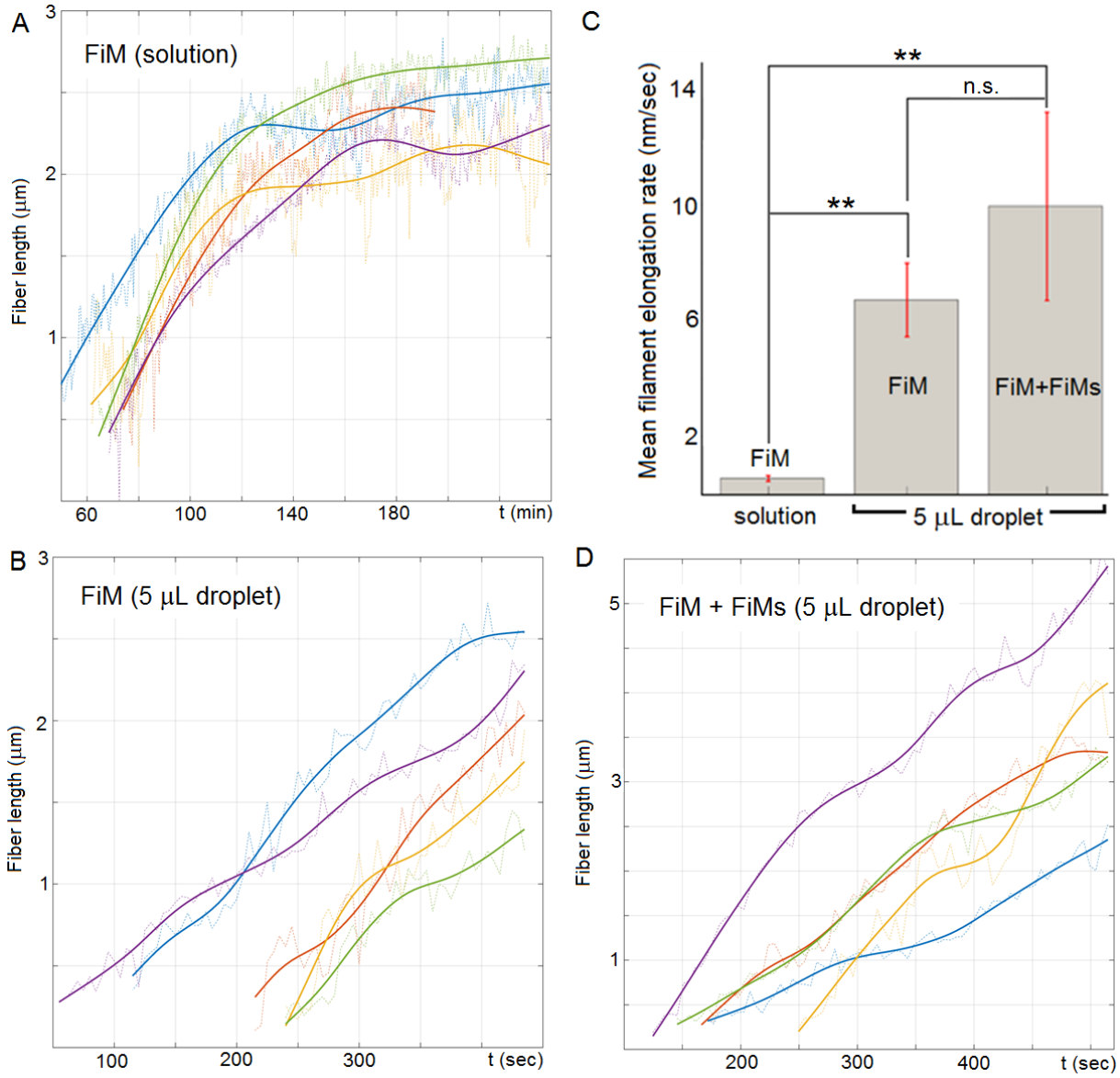

Figure S2. Elongation kinetics for individual FiM filaments assembled (A) in a static (equilibrated) solution and (B) near the contact line of a drying sessile droplet. (C) Mean filament elongation rates during the linear phase of FiM assembly under different conditions. Error bars denote standard deviations, with statistical significance assessed using a two-sided t-test with unequal variances and a two-sided Wilcoxon rank sum test. Differences are represented with ** for $p < 0.01$ (significant) and n.s. for $p > 0.05$ (not significant): elongation rates for FiM assembled in solution were significantly lower than those of filaments assembled in the droplet. (D) Elongation kinetics for individual filaments assembled from FiM and FiMs (1:1 molar ratio) in a star structure near the contact line of a drying sessile droplet. Solid lines in A, B, and D show spline fits applied to raw data (dashed lines).

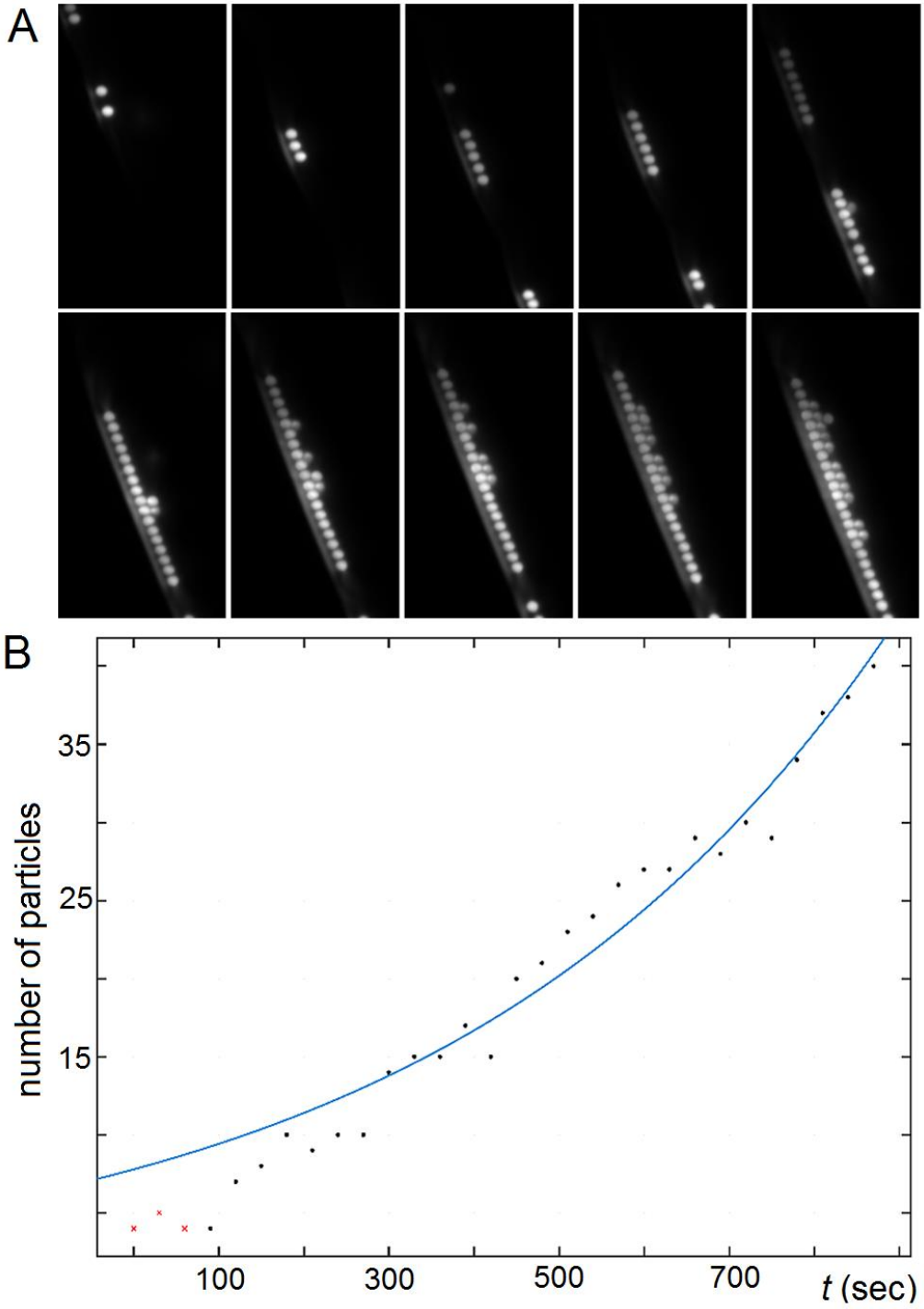

Figure S3. **A coffee-ring growth by non-hierarchical systems**. (A) time-lapse imaging of 1 μm fluorescent microspheres in water with individual images taken at 1.5 min intervals. (B) Observed increase in the number of particles in the ring and exponential fit to the data over the first 15 minutes after droplet deposition. Key: number of particles included in and excluded from calculations are shown as black dots and red crosses, respectively; the blue curves is a fit for included particles.

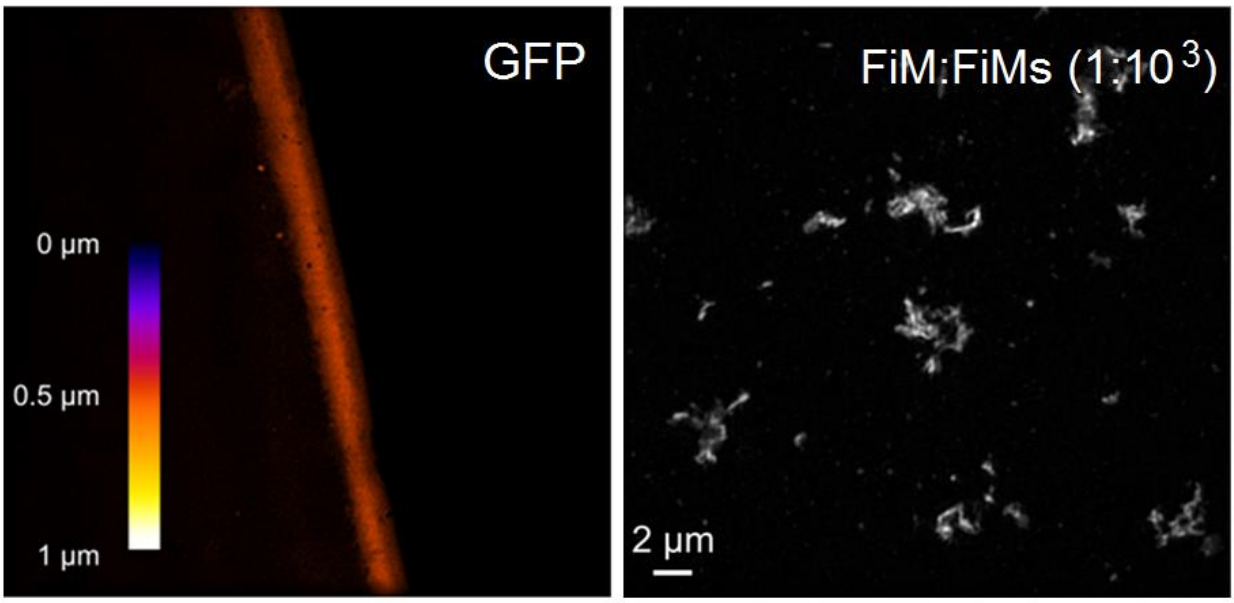

Figure S4. **A coffee ring growth by non-assembling protein systems**. Color-coded depth projections of the contact lines of droplets (5 µL) dried over 30 min for enhanced green fluorescent protein (left, GFP) and FiM:FiM-Alexa Fluor 488 ($1:10^{-3}$ molar ratio) mixed with FiMs at $1:10^{3}$ ratio (right). Color scale bar is 1 µm.